

Effects of atomic ordering on the electronic and optical properties of self-assembled $\text{In}_x\text{Ga}_{1-x}\text{As}/\text{GaAs}$ semiconductor quantum dots

Ranber Singh and Gabriel Bester

Max-Planck-Institut für Festkörperforschung, Heisenbergstrasse 1, 70569 Stuttgart, Germany

(Received 2 August 2011; revised manuscript received 30 November 2011; published 14 December 2011)

We study the effect of atomic ordering on the electronic and optical properties of $\text{InGaAs}/\text{GaAs}$ semiconductor nanostructures via atomistic empirical pseudopotentials. We find that ordering sharply increases the polarization anisotropy and the fine structure splittings, and we explain the underlying physics. We suggest that ordering may be responsible for some experimental results where large values of these observables have been reported. We show that ordering pins the polarization into a certain direction that remains robust upon elongation of the structure—a fact that may be advantageous for use as polarized light sources.

DOI: [10.1103/PhysRevB.84.241402](https://doi.org/10.1103/PhysRevB.84.241402)

PACS number(s): 78.67.Hc, 61.66.Dk, 73.21.La, 81.07.Ta

The phenomenon of spontaneous ordering in ternary alloy semiconductors $\text{A}_x\text{B}_{1-x}\text{C}$ has been extensively studied from the mid 80's to the early 90's¹⁻⁷ and has led to a solid understanding of the physics involved. It was shown that a prevalent type of ordering for [001] crystal growth is the CuPt-type ($L1_1$ structure), where the $\{111\}$ planes are fully occupied by either A , B , or C atoms. Deviations from this long-range order can be quantified by the degree of ordering η . Generally, an $\text{In}_x\text{Ga}_{1-x}\text{As}$ alloy consists of alternating (111) layers of $\text{In}_{(x+\eta/2)}\text{Ga}_{(1-x-\eta/2)}$, pure As, and $\text{In}_{(x-\eta/2)}\text{Ga}_{(1-x+\eta/2)}$. For $\eta = 1$, the (111) planes are either Ga-pure or In-pure, while $\eta = 0$ corresponds to a random distribution. While this long-range order is well known in bulk alloy structures and there exists some level of control to achieve or suppress ordering via growth conditions, ordering that may develop inside a nanostructure is a recent topic. Some recent experiments⁸⁻¹⁰ have evidenced ordering in nanostructures, although it remains a difficult task. The volume of a self-assembled quantum dot (QD) is only very small compared to the volume of the sample and hence difficult to see via, e.g., x-ray diffraction. Arguments for the existence of ordered phases in QDs can be given from thermodynamics.⁹ It is also known that extreme strain conditions, as given in a QD, may favor ordering.¹¹ Besides the arguments based on growth, we noticed in the optical properties of QDs two facts that elude a quantitative theoretical description: the measurements of very large fine-structure splittings¹²⁻¹⁴ and optical anisotropies.¹⁵ It seems that the variations in shape, size, or composition, we can assume theoretically, are not able to bring theory and experiment in agreement. One avenue that has not been explored is the influence of ordering on the QD's electronic and optical properties. We undertook this task and show that ordering leads to a low symmetry point group C_S where the dot-filling material lacks $[110]$ - $[\bar{1}\bar{1}0]$ symmetry. This is in contrast to nonordered QDs where this symmetry is only broken via the interfaces. The main consequences are: a closing of the band gap due to biaxial strain, an increased light-hole character in the first hole state, very significant increase in the optical polarization anisotropy, and fine structure splittings. We compare the atomistic long-range order effect and the shape elongation effect.

We consider different self-assembled lens-shaped $\text{In}_{0.5}\text{Ga}_{0.5}\text{As}/\text{GaAs}$ QDs with circular and elliptical bases. We

have chosen $x = 0.5$ to be able to vary η from zero to one. The circular QDs have a diameter of 20 nm and a height of 3.5 nm. The elongation is defined as the ratio of elliptic axis along the $[110]$ and $[\bar{1}\bar{1}0]$ crystal directions, while keeping the volume constant. The structures are relaxed to minimize the strain energy using the valence force field method. The single particle orbitals and energies of the QDs are calculated using the atomistic pseudopotential approach,^{16,17} taking strain, band coupling, coupling between different parts of the Brillouin zone, and spin-orbit coupling into account. The simulation cells contain about three million atoms. The Coulomb and exchange integrals are calculated from the atomic wave functions,¹⁸ and the correlated excitonic states are calculated by the configuration interaction¹⁹ using all possible determinants constructed from the twelve lowest (highest) energy electron (hole) states, thus accounting for correlations.

In the bulk zinc-blende material, with T_d point group symmetry, the CuPt-type ordering reduces the symmetry to C_{3v} (a piezo- and pyroelectric point group). This is also the symmetry of a $[111]$ grown superlattice. Indeed, this type of ordering can be viewed as a short period $[111]$ superlattice. It was shown²⁰ that CuPt-type ordering leads to a Hamiltonian analogous to the one obtained in the case of strain along the $[111]$ direction. The degenerate heavy- and light-hole valence band states split due to ordering in qualitatively the same way they split under $[111]$ strain. Unlike the case of $[001]$ strain, where the splitting is due to the biaxial strain, the $[111]$ splitting is a result of shear strain only. In a nanostructure, the symmetry is a direct product of the atomistic symmetry and the symmetry reduction brought about by the interface. For a T_d zinc-blende material with an interface such as the one encountered in self-assembled dots (e.g., lens-shaped), the symmetry is reduced to C_{2v} . This latter reduction makes the $[110]$ and the $[\bar{1}\bar{1}0]$ directions inequivalent (they are equivalent in the T_d bulk). In the case of the ordered structure, we start from a C_{3v} atomistic symmetry, and the interfaces, i.e., the macroscopic shape, reduce it to C_S , with only one reflection plane. In Fig. 1, we show two side views of the (110) and $(\bar{1}\bar{1}0)$ planes cut through the center of a QD with (111) CuPt-like ordering. The red, blue, and black circles represent the In, Ga, and As atoms, respectively. It is important to notice that the (110) plane shows inversion symmetry while no such symmetry exists in the $(\bar{1}\bar{1}0)$ plane.

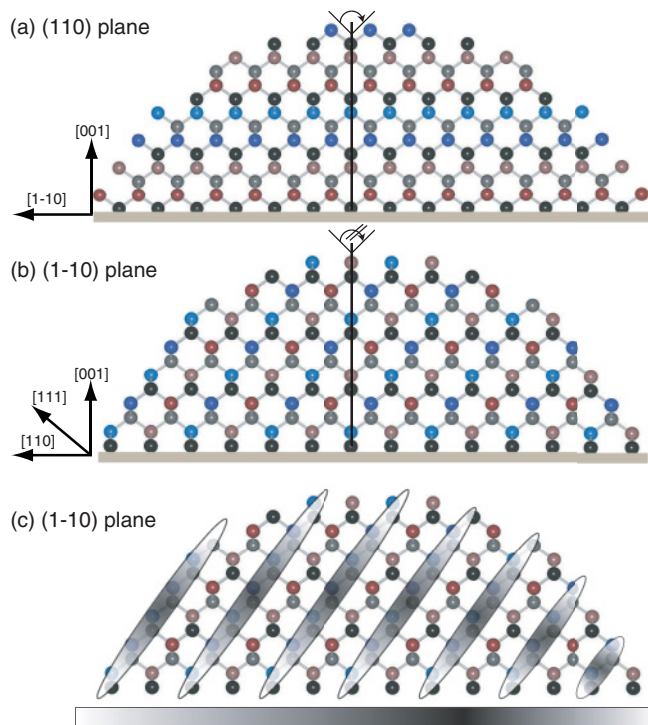


FIG. 1. (Color) The (a) (110) and (b),(c) ($\bar{1}\bar{1}0$) planes cut through the center of a QD with CuPt-type ordering. The red, blue, and black circles represent the In, Ga, and As atoms, respectively, in the front surface layer, while light-colored red, blue, and black circles represent the corresponding atoms one atomic layer beneath the surface. A schematic for the localization of holes is shown in (c).

The single particle energies of the first electron state e_0 and the first three hole states $h_{0,1,2}$ as a function of η are given in Fig. 2(a). The energies of electron states are rather insensitive to ordering, while hole states show a significant blueshift. The closing of the band gap with ordering is well known for semiconductor alloys.^{7,21–23} However in the bulk-alloy, this closing is driven by shear strain that splits heavy- and light-hole states,²⁰ while in the QD, we find the change in biaxial strain to be the dominant factor. In the QD, the heavy- and light-hole states are strongly split by confinement and by the biaxial strain resulting from the pseudomorphic growth. Ordering increases the amount of biaxial strain, and this occurs through the interface. The electron states are insensitive to volume conserving strains, in a first approximation, and exhibit no significant shift. We also notice an energetic splitting of the hole P states $h_{1,2}$ that we will discuss based on an analysis of the wave functions.

In Fig. 3(a), we plot the state densities of S (h_0) and P (h_1, h_2) hole states for varying η . The white crosses mark the center of the dot and show that the hole states shift toward the $[\bar{1}\bar{1}0]$ direction with increasing η . From the previous symmetry analysis [Figs. 1(a) and 1(b)], we know that a broken symmetry along the $[110]$ direction (no mirror plane) is formally expected. There is, however, a less formal and more intuitive view to understand this result. The hole wave functions are mainly localized on the As atoms with some contributions on the In atoms. Localization of holes on Ga

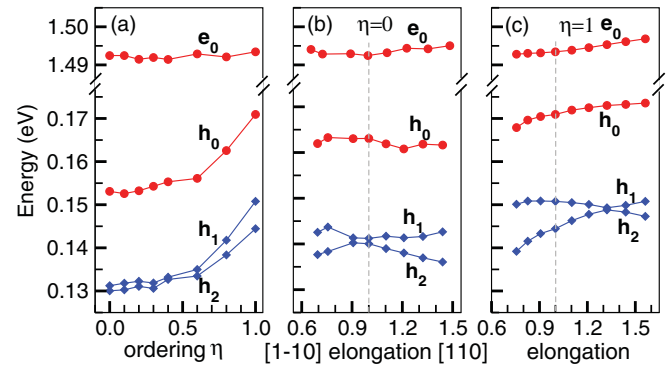


FIG. 2. (Color online) Single particle energies (with respect to the vbm of GaAs) of electron e_0 and hole $h_{0,1,2}$ states as a function of the degree of ordering (a) in a circular base QD and as a function of base elongation for $\eta = 0$ (b) and $\eta = 1$ (c).

is maximally avoided. The existence of pure As, In, and Ga (111) planes offers to the holes the possibility to localize in extended In-As layers partly avoiding Ga layers. This situation is depicted in Fig. 1(c), where the gray stripes represent the hole density. These holes are mobile within these planes and will minimize their kinetic energy by delocalizing as much as possible within the planes, i.e., the density is highest at the geometric center of each plane. This layered structure, together with the QD's shape, leads to the shift along $[\bar{1}\bar{1}0]$. The effect on electron states (shown with a lighter color in Fig. 3) is less pronounced because of their rather small effective mass and their inability to be localized on the atomic scale.

We further analyze in Fig. 4 the hole wave functions $h_{0,1,2}$ in terms of their Bloch function character by projecting them onto heavy- and light-hole bulk states (see, e.g., Ref. 18). The hole states have in general a dominant heavy-hole character (80–93%) as a result of confinement and biaxial strain. Indeed, heavy holes with their purely “in-plane” orbital character, $\mp \frac{1}{\sqrt{2}}(|x\rangle \pm i|y\rangle)$, are favorable in the QD geometry with strong confinement in the growth z direction. Accordingly, light holes, with their contributions from the Bloch z band, have reduced contributions. The intuitive picture drawn in Fig. 1(c) suggests that the holes in the ordered structure, with their localization on “upwards” planes, should have an increase of the z , and hence light-hole, contribution, compared to the

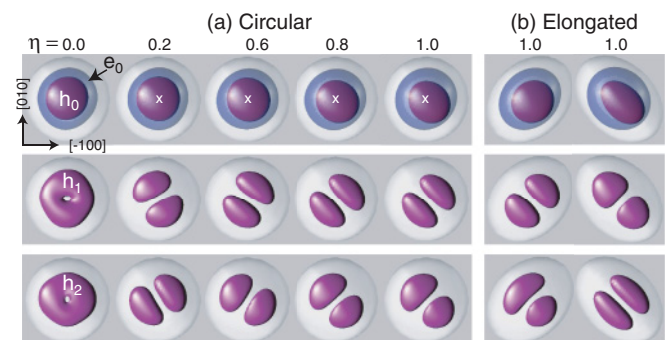


FIG. 3. (Color online) Square of the wave functions for different ordering parameters for QDs with circular base (a) and for elongated QDs with elongation 0.76 and 1.32 (b). The isosurfaces enclose 75% of the probability densities.

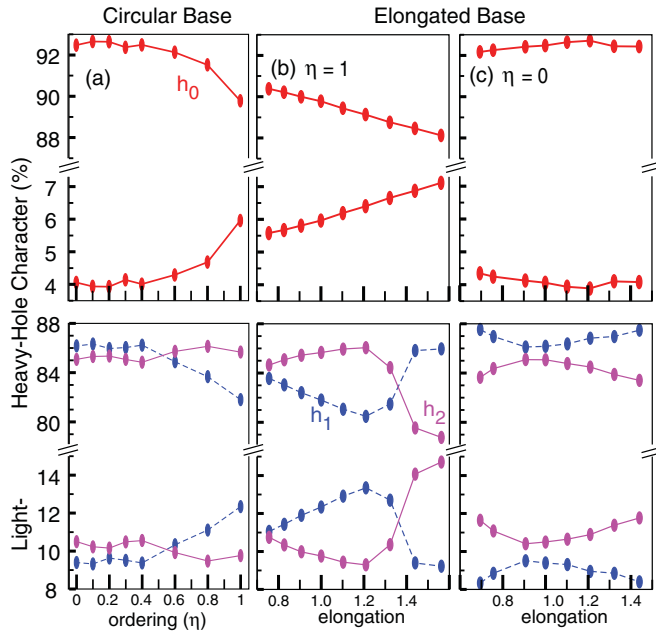


FIG. 4. (Color online) Heavy- and light-hole characters of S and P hole states as a function of η in a QD with circular base (a) and with elongated base for $\eta = 1$ (b) and $\eta = 0$ (c).

random alloy case. This is precisely the result of the analysis in Fig. 4(a), showing growing light-hole contributions with increasing order. From Fig. 3(a), we know that (111) ordering favors the P state with lobes oriented along the $[1\bar{1}0]$ direction. From Fig. 4(a), we see that this state (h_1) significantly increases its light-hole character with increasing ordering (like the hole S state h_0). The second hole P state h_2 has nearly constant heavy-hole and light-hole characters as the node along the $[110]$ direction inhibits the expansion of the wave function along the planes.

Since the ordering further breaks the $[110]$ - $[1\bar{1}0]$ symmetry, it is interesting to contrast this atomistic effect with the macroscopic effect of the QD elongation. We show the single particle energies as a function of QD elongation for the random alloy in Fig. 2(b) and the fully ordered alloy in Fig. 2(c). For this volume-conserving elongation, the energy shifts are generally small. The most significant feature is the anticrossing and the crossing of the hole P states $h_{1,2}$ for $\eta = 0$ and $\eta = 1$, respectively. As already seen in Fig. 3(a), ordering favors the P states elongated along the $[1\bar{1}0]$. So a QD elongation along this direction (elongation < 1) will further split the P states, while an elongation along $[110]$ will reduce the splitting until the states eventually cross, in our case for an elongation of 1.32. For a random alloy, the states anticross, since they have the same symmetry (Γ_1) for an elongation around 1. In Fig. 3(b), we show the results for $\eta = 1$ and two large elongations, 0.76 and 1.44. In both cases, the hole states follow the elongation. However for elongations between 1.0 and 1.32 ordering wins, i.e., the state h_1 is oriented along $[1\bar{1}0]$ although the dot is elongated along $[110]$. The analysis of the heavy- and light-hole character is given as a function of elongation in Figs. 4(b) and 4(c). For the hole S state h_0 , the light-hole character increases in case there is ordering [Fig. 4(b)], but not for the random alloy case [Fig. 4(c)]. So,

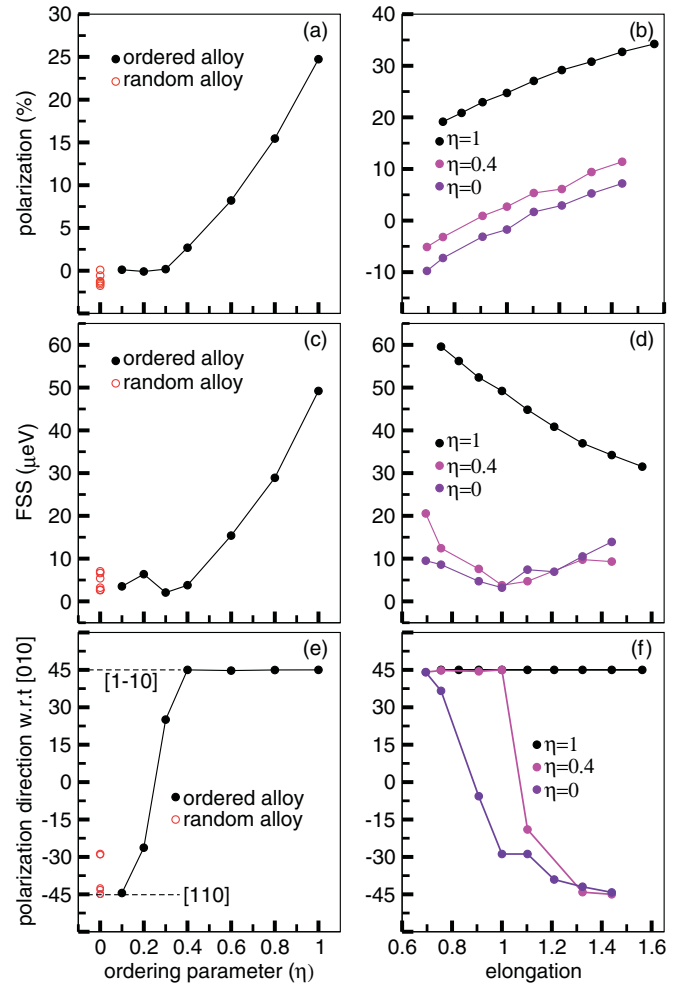


FIG. 5. (Color online) (a),(b) Total polarization of the exciton emission, (c),(d) fine structure splitting, (e),(f) polarization direction of the lowest energy bright exciton state. All given for different ordering parameters (a),(c),(e) and elongations (b),(d),(f).

for elongation to influence the light-hole character of the h_0 state, atomic ordering is required. For the hole P states and $\eta = 1$, we see that the P state with a node along $[1\bar{1}0]$ (h_2 for elongation > 1.32 and h_1 for elongation < 1.32) shows a significant increase of light-hole character. The orthogonal state with node along $[110]$ has a nearly constant heavy- and a nearly constant light-hole character.

We further investigated the effect of atomic ordering on the optical properties in Fig. 5. In Figs. 5(a) and 5(b), we show the polarization of the excitonic transition defined as $(I_{110} - I_{1\bar{1}0}) / (I_{110} + I_{1\bar{1}0})$, where I_{110} and $I_{1\bar{1}0}$ are the intensities of the excitonic emission (summing both bright states) polarized along $[110]$ and $[1\bar{1}0]$. Using an envelope function description, polarization anisotropy is understood in the following terms: The hole states are composed of several envelope functions $|\phi_x\rangle, |\phi_y\rangle, |\phi_z\rangle$, each associated with a Bloch function $|x\rangle, |y\rangle, |z\rangle$ (where $|x\rangle$ could be oriented along the $[110]$ direction). The electron is described by a single envelope function $|\phi_s\rangle$ (to a good approximation). The oscillator strength is given by the overlap of the hole and electron envelope function. If a dot is elongated along x , then the hole's

$|\phi_x\rangle$ -envelope function contribution increases, compared to the contribution from $|\phi_y\rangle$. For such an elongated QD, the intensity $I_X \propto |\langle \phi_x | \phi_s \rangle|^2$ is larger than $I_Y \propto |\langle \phi_y | \phi_s \rangle|^2$, leading to nonzero anisotropy. This leads to the nearly-linear slopes in Fig. 5(b). In an envelope function description (k,p), this is the only effect that leads to anisotropy, and for a random alloy, it is in the range of -10 to $+10\%$ [Fig. 5(b)]. In Fig. 5(a), we show the effect of the atomic ordering on the polarization. This purely atomistic effect can boost up the polarization to 25%. It cannot be understood in terms of the envelope functions, visible in Fig. 3, but from the symmetry of the Bloch functions.

In Figs. 5(c)–5(f), we study the optical properties related to the individual exciton bright states. These two states are split by the electron-hole exchange interaction, and we calculate it according to Ref. 18. In Figs. 5(c) and 5(d), we plot the fine-structure splitting (FSS) for varying η and elongations. For $\eta = 0$, we plot the FSS for different random alloy realization and obtain FSS between 3 and 8 μeV . For increasing ordering, the FSS increases significantly to 50 μeV . An influence of η on the FSS is not surprising: The FSS represents the inequivalence between the [110] and $[1\bar{1}0]$ directions.¹⁸ For a random alloy, this inequivalence is a rather subtle effect that has two origins. One is an asymmetry in the interfaces of the QD's²⁴ (much like in a quantum well, where interfaces can lower the overall symmetry) that propagates from the interface to the dot center via strain.²⁴ The second is the random alloy fluctuations that influences the hole states significantly¹⁸ and favor a certain, random direction for the polarization of the lowest exciton state. In most of the cases, the first effect, that favors [110] polarization, prevails, and we obtain [110] polarized lowest exciton states. But in some cases, the

second effect dominates, and the polarization is randomly oriented. The situation for the ordered alloy is much simpler: Through atomic CuPt-type ordering, the bulk material has C_{3v} symmetry, with inequivalent [110] and $[1\bar{1}0]$ directions. This inequivalence does not require asymmetries in remote interfaces but is atomistically intrinsic.

To fully understand the nonmonotonic dependences in Figs. 5(c) and 5(d), we show in Figs. 5(e) and 5(f) the polarization direction of the lower exciton state. The random alloy favors the [110] polarization, with some exceptions shown by the open circles. This polarization is quickly rotated to the $[1\bar{1}0]$ direction by an increasing η . In Fig. 5(f), we show that the elongation smoothly rotates the polarization for a random alloy. For $\eta = 1$, however, even large elongations fail to change the polarization direction of the lowest exciton state. The robustness of the polarization direction could be exploited experimentally to isolate the effect of the ordering. While the polarization direction rotates smoothly with applied external electric²⁵ or strain fields,^{26,27} it should remain locked for ordered QDs.

In summary, we investigate the effect of atomic ordering on the electronic and optical properties of $\text{In}_x\text{Ga}_{1-x}\text{As}/\text{GaAs}$ self-assembled quantum dots. We find that ordering leads to large fine-structure splittings and large optical anisotropies, and we suggest that it could explain experimental results that remained unmatched by theory until now. Concluding, we shall remark that ordering may be seen as a disadvantage if QDs with small fine-structure splittings are the target, but ordering also favorably removes the uncertainty in fine-structure splittings, optical anisotropies, and polarization directions encountered in QDs made of random alloys. Ordering may therefore represent a new avenue to obtain robust polarized photon sources.

¹A. Zunger and S. Mahajan, *Handbook on Semiconductors*, Vol. 3 (Elsevier Science B. V., Amsterdam, 1994).

²*Spontaneous Ordering in Semiconductor Alloys*, edited by A. Mascarenhas, (Kluwer Academic/Plenum Publishers, New York, 2002).

³T. S. Kuan, T. F. Kuech, W. I. Wang, and E. L. Wilkie, *Phys. Rev. Lett.* **54**, 201 (1985).

⁴G. P. Srivastava, J. L. Martins, and A. Zunger, *Phys. Rev. B* **31**, 2561 (1985).

⁵M. A. Shahid, S. Mahajan, D. E. Laughlin, and H. M. Cox, *Phys. Rev. Lett.* **58**, 2567 (1987).

⁶G. Stringfellow and G. Chen, *J. Vac. Sci. Technol. B* **9**, 2182 (1991).

⁷P. Ernst, C. Geng, F. Scholz *et al.*, *Appl. Phys. Lett.* **67**, 2347 (1995).

⁸U. Hakanson, V. Zwiller, M. Johansson *et al.*, *Appl. Phys. Lett.* **82**, 627 (2003).

⁹P. Moeck, *Nonlinear Analysis* **63**, e1311 (2005).

¹⁰A. Malachias, T. U. Schüllli, G. Medeiros-Ribeiro, L. G. Cancado, M. Stoffel, O. G. Schmidt, T. H. Metzger, and R. Magalhaes-Paniago, *Phys. Rev. B* **72**, 165315 (2005).

¹¹L. K. Teles, L. G. Ferreira, L. M. R. Scolfaro, and J. R. Leite, *Phys. Rev. B* **69**, 245317 (2004).

¹²R. Seguin, A. Schliwa, S. Rodt, K. Potschke, U. W. Pohl, and D. Bimberg, *Phys. Rev. Lett.* **95**, 257402 (2005).

¹³J. J. Finley, D. J. Mowbray, M. S. Skolnick, A. D. Ashmore, C. Baker, A. F. G. Monte, and M. Hopkinson, *Phys. Rev. B* **66**, 153316 (2002).

¹⁴M. Bayer, G. Ortner, O. Stern *et al.*, *Phys. Rev. B* **65**, 195315 (2002).

¹⁵I. Favero, G. Cassabois, A. Jankovic *et al.*, *Appl. Phys. Lett.* **86**, 041904 (2005).

¹⁶L.-W. Wang and A. Zunger, *Phys. Rev. B* **59**, 15806 (1999).

¹⁷G. Bester, *J. Phys. Condens. Matter* **21**, 023202 (2009).

¹⁸G. Bester, S. Nair, and A. Zunger, *Phys. Rev. B* **67**, 161306(R) (2003).

¹⁹A. Franceschetti, H. Fu, L.-W. Wang, and A. Zunger, *Phys. Rev. B* **60**, 1819 (1999).

²⁰S.-H. Wei and A. Zunger, *Phys. Rev. B* **49**, 14337 (1994).

²¹A. Gomyo, T. Suzuki, and S. Iijima, *Phys. Rev. Lett.* **60**, 2645 (1988).

²²S. Kurtz, J. Olson, and A. Kibbler, *Appl. Phys. Lett.* **54**, 718 (1989).

²³T. Kanata, M. Nishimoto, H. Nakayama, and T. Nishino, *Phys. Rev. B* **45**, 6637 (1992).

²⁴G. Bester and A. Zunger, *Phys. Rev. B* **71**, 045318 (2005).

²⁵A. J. Bennett *et al.*, *Nat. Phys.* **6**, 947 (2010).

²⁶J. D. Plumhof *et al.*, *Phys. Rev. B* **83**, 121302(R) (2011).

²⁷R. Singh and G. Bester, *Phys. Rev. Lett.* **104**, 196803 (2010).